Since January 2020 Elsevier has created a COVID-19 resource centre with free information in English and Mandarin on the novel coronavirus COVID-19. The COVID-19 resource centre is hosted on Elsevier Connect, the company's public news and information website.

SARS-CoV-2 Spike Protein in Intestinal Cells of a Patient with Coronavirus Disease 2019 Multisystem Inflammatory Syndrome

Juan Mayordomo-Colunga, MD, PhD[1,2,3], Ana Vivanco-Allende, MD, PhD[1,2], Inés López-Alonso, PhD[2,3,4], Cecilia López-Martínez, MSc[2,3], Iván Fernández-Vega, MD, PhD[5], Helena Gil-Peña, PhD[1,2], and Corsino Rey, MD, PhD[1,2,6,7]

A previously healthy 12-year-old boy had severe acute respiratory syndrome coronavirus 2 (SARS-CoV-2)-related multisystem inflammatory syndrome (MIS-C) that was rapidly fatal. Autopsy revealed the presence of a large intracardiac thrombus. SARS-CoV-2 spike protein was detected in intestinal cells, supporting the hypothesis that viral presence in the gut may be related to the immunologic response of MIS-C. *(J Pediatr 2022;243:214-8).*

Multisystem inflammatory syndrome associated with severe acute respiratory syndrome coronavirus 2 (SARS-CoV-2) infection (MIS-C) was described during the first SARS-CoV-2 pandemic wave in Europe.[1] Days or weeks after SARS-CoV-2 infection or exposure, some children (predominantly school-aged) develop this life-threatening disease.[2] Patients present with fever, gastrointestinal symptoms, high levels of inflammatory markers, and cardiogenic shock.[2-4] Although the pathophysiology remains unclear, MIS-C encompasses cytokine-mediated hyperinflammation.[5] A requirement for intensive care is reported in 50%-80% of cases of MIS-C, and the fatality rate is 0-2%.[2,4-9] In the 3 reported pediatric autopsies, SARS-CoV-2 was found in several tissues, and in intestinal cells in 1 child.[10] Here we present a case of overwhelming MIS-C in a previously healthy child, providing relevant information about autopsy findings and histologic, immunohistochemical, and immunofluorescent analysis for SARS-CoV-2.

Case Presentation

A 12-year-old boy with no significant past medical history presented with symptoms that began 3 days before admission consisting of malaise, fever, maculopapular rash, and diffuse abdominal pain, with diarrhea. Two family members had tested positive for SARS-CoV-2 by reverse-transcriptase polymerase chain reaction on nasopharyngeal swab 6 weeks earlier. At presentation, the patient tested negative for SARS-CoV-2 by reverse-transcriptase polymerase chain reaction on nasopharyngeal swab but positive for serum SARS-CoV-2 immunoglobulin G.

Abdominal ultrasound showed inflammation of the terminal ileum and peritoneal free fluid inconsistent with appendicitis. Amoxicillin-clavulanate acid and intravenous fluids were started. Microscopic urinalysis showed no leukocytes or nitrates, although a sample sent for culture revealed the presence of 50 000 CFU/mL of *Providencia stuartii*. Blood cultures and subsequent tracheal aspirate cultures were negative.

Several hours after admission, the patient developed fluid-refractory shock and was transferred to a pediatric intensive care unit (PICU). Initial tests revealed lymphopenia and increased levels of inflammatory markers (**Table I**; available at www.jpeds.com). Dopamine was begun, and the patient was intubated and subsequently treated with adrenaline and milrinone. Antibiotic coverage was changed to cefotaxime and clindamycin. MIS-C was considered a possible diagnosis, and he was given corticosteroids (methyl-prednisolone 50 mg/12 hours, ~1.7 mg/kg/day). Echocardiography performed after intubation in the PICU showed a slight reduction in left ventricular ejection fraction (~60%), with no other obvious abnormalities. Blood tests showed progressive increases in levels of inflammatory markers (**Table I**).

The next day, the child developed a fever up to 42.1°C and was unresponsive to intravenous immunoglobulin and a 1-g methyl-prednisolone pulse, necessitating the addition of noradrenaline to maintain blood pressure. Low molecular weight heparin was started, and antibiotic therapy was changed to vancomycin and meropenem. Levels of serum creatinine, procalcitonin, D-dimer, lactate dehydrogenase, and cardiac markers showed abrupt elevations (**Table I**). The echocardiogram was repeated, demonstrating a left ventricular ejection fraction of ~50%, without any other anomalies. At 8 hours after this second echocardiogram (45 hours after PICU admission), the child developed

MIS-C	Multisystem inflammatory syndrome associated with SARS-CoV-2 infection
PICU	Pediatric intensive care unit
SARS-CoV-2	Severe acute respiratory syndrome coronavirus 2

From the [1]Department of Pediatrics, Hospital Universitario Central de Asturias, Oviedo, Spain; [2]Instituto de Investigación Sanitaria del Principado de Asturias, Oviedo, Spain; [3]Centro de Investigación Biomédica En Red–Enfermedades Respiratorias, Instituto de Salud Carlos III, Madrid, Spain; [4]Instituto Universitario de Oncología del Principado de Asturias, Oviedo, Spain; [5]Department of Pathology, Hospital Universitario Central de Asturias, Oviedo, Spain; [6]Department of Pediatrics, University of Oviedo, Oviedo, Spain; and [7]Maternal and Child Health and Development Research Network, Institute of Health Carlos III, Madrid, Spain

C.L.-M. is funded by the Ministerio de Universidades, Spain (Grant FPU18/02965), which had no role in the study design, data analysis, manuscript preparation, or the decision to submit the manuscript. The authors declare no conflicts of interest.

Portions of this study were presented at the European Society of Pediatric and Neonatal Intensive Care, June 15-18, 2021 (virtual).

https://doi.org/10.1016/j.jpeds.2021.11.058

Table II. Main macroscopic and histopathologic findings of systems/organs observed

Macroscopic findings	Microscopic findings	
Respiratory system: Lung		
Severe lung congestion, with petechiae on the external surface; no thrombi in the pulmonary artery or main branches	Alveoli	Enlarged pneumocytes with large nuclei, type II pneumocyte hyperplasia, focal sloughing, intra-alveolar hemorrhage; no evidence of intra-alveolar neutrophil infiltration, amphophilic granular cytoplasm, or viral cytopathic-like changes; no hyaline membranes identified
	Vessels	Edematous and congested vessels and hyaline thrombi in microvessels; no deposits of complement C4d in the microvasculature noted
	Cellular components	No presence of syncytial giant cells or infiltration of immune and inflammatory (lymphocytes and monocytes); mild increase in stromal cells
Urinary system: Kidney		
Visible clots in calices; no signs consistent with pyelonephritis	Glomerulus	Ischemic changes, podocyte vacuolation, and accumulation of plasma in Bowman space
	Renal tubules	Nonisometric vacuolar degeneration and edematous epithelial cells; focal interstitial hemorrhage
	Vessels	Erythrocyte aggregates obstructing the lumen of capillaries without platelet or fibrinoid material, fibrin thrombus, and shrinkage of capillary loops in glomeruli
Gastrointestinal system		
Edematous cecum mucosa. A 9 × 2.5 cm lymphadenopathy found next to the cecum, which on cut sections revealed extensive areas of hemorrhage	Colon	Numerous infiltrating plasma cells and lymphocytes with interstitial edema in the lamina propria; intense edema of submucosa with mild infiltration of immune cells; significant deposits of complement C4d in the microvasculature; arteriolar microthrombi
Severe liver congestion	Liver	Focal macrovesicular steatosis, nuclear glycogen accumulation in hepatocytes, moderate zone 3 sinusoidal dilatation with extensive centrilobular necrosis (submassive hepatic necrosis)
No other significant macroscopic findings in other parts of the gastrointestinal system	Esophagus	No significant changes
	Stomach	Partial epithelial degeneration, necrosis, and shedding of the gastric mucosa. Dilatation and congestion of small blood vessels; moderate edema of submucosa with mild infiltration of immune cells (as lymphocytes, monocytes, and plasma cells)
	Pancreas	No significant changes
Cardiovascular system		
Nondilated heart showing a 4 × 1 cm thrombus in the right ventricle, encircling a papillary muscle; patent coronary arteries	Heart	Significant interstitial edema and presence of inflammatory cells; foci of lymphocytic inflammation $CD3^+$; presence of diffuse mobilization and infiltration by $CD68^+$ macrophages in the myocardium; significant deposits of complement C4d in the microvasculature; no signs of vasculitis in coronary arteries; microscopy normal
Reproductive system		
No significant changes		
Nervous system		
No significant changes		
Skin		
Macular rash mainly in the dorsum, with occasional petechiae	Vessels: Perivascular inflammatory cells, intraluminal thrombi; significant deposits of complement C4d in the microvasculature	
	Epidermis: no significant alterations	
Bone marrow		
	Intense hemophagocytosis	
Skeletal muscle		
	Focal myonecrosis	

pulseless ventricular tachycardia and did not respond to cardiopulmonary resuscitation.

At autopsy, macroscopically the heart was nondilated and had a 4 × 1 cm thrombus in the right ventricle, encircling a papillary muscle (**Figure 1**, A; available at www.jpeds.com). Other macroscopic findings are shown in **Figure 1** and described in **Table II**. Disseminated intravascular coagulopathy was identified in most organs. Severe inflammation was found in the intestine and the heart, and hemophagocytosis was prevalent in the bone marrow (**Figure 2**; available at www.jpeds.com). Complement C4d deposits were found in microvessels of the intestine, skin, liver, and heart (**Figure 3**; available at www.jpeds.com), but not in other organs.

To perform immunofluorescence, tissue slices were deparaffinated and antigens retrieved in citrate buffer 0.1 M (pH 6). Autofluorescence was diminished using Sudan black saturated solution for 30 minutes. Slides were then washed with phosphate-buffered saline (PBS), permeabilized with 0.1% Triton X-100 in PBS for 15 minutes, and blocked with 1% bovine serum albumin in PBS. Slides were then incubated overnight at 4°C with a rabbit monoclonal antibody against SARS-CoV-2 spike protein (Invitrogen) at 1:100 dilution. The next day, slides were incubated with the corresponding secondary fluorescent antibody (donkey IgG Alexa Fluor 594-conjugated anti-rabbit; Thermo Fisher Scientific) at room temperature for 45 minutes. Slides were coverslipped

with SlowFade Diamond Mountant with DAPI (Invitrogen) for nuclear visualization. Immunofluorescence detected the presence of protein S (spike) in the intestine (**Figure 4**) and in a positive control sample (**Figure 5**; available at www.jpeds.com). Spike protein could not be identified in the heart, lungs, or enlarged pericecal lymph node (**Figure 6**; available at www.jpeds.com).

Discussion

The most relevant observation in the present case is the presence of spike protein in intestinal cells in a child with MIS-C. In reports of autopsies of children with MIS-C, intestinal cells were studied in only 1 subject, revealing the presence of SARS-CoV-2 components in the intestinal epithelium.[10]

Our case has some unique features, mainly the overwhelming evolution in <48 hours, refractory hyperpyrexia, and cardiac thrombus. The child met all the current criteria for MIS-C, but because many clinical features are common with bacterial septic shock, broad-spectrum antibiotics were used. The formation of a large cardiac thrombus is noteworthy, as this is an uncommon complication in MIS-C.[11] Arrythmia has been one of the most frequently reported cardiovascular complications in MIS-C,[7] and ventricular tachycardia has been reported as well.[9]

Histologic examination revealed frequent extensive thrombosis and areas of hemorrhage in most organs, findings indistinguishable from other causes of disseminated intravascular coagulopathy. Duarte-Neto et al also reported thrombi in most organs of patients with MIS-C; inflammation was present mainly in the heart and the intestine, and inflammation was described in most organs in their case series.[10] We cannot exclude the possibility that the short time from our patient's onset of symptoms to death could be related to limited sites of inflammation. However, given that immune activation may be primarily responsible for tissue damage, there could be a discrepancy between the presence of virus and tissue inflammation, as has been described in adults with fatal coronavirus disease 2019 (COVID-19).[12]

MIS-C has some clinical similarities with Kawasaki disease, although they appear to be distinct entities.[13] Histologically, systemic vasculitis is the main feature in Kawasaki disease, affecting the coronary arteries in most patients. Furthermore, inflammation is present in most organs and tissues in fatal Kawasaki disease.[14] In contrast, in our case, inflammation was confined to the heart and the gut, and vasculitis was not found. Moreover, infiltration of coronary arteries was not found in our case or in other reported fatal cases of MIS-C.[10,15]

Neither diffuse alveolar damage nor hyaline membrane formation was present in our case or in other reported cases of MIS-C, except for some foci of exudative diffuse alveolar damage in 1 child.[10] These findings are consistent with the lack of respiratory symptoms at presentation of our patient, as well as the relative paucity of respiratory involvement described in MIS-C.[16] The lungs in our case and in previously reported cases showed congestion, edema, and foci of hemorrhage and thrombi.[10] Conversely, the lungs in 2 patients with a pulmonary form of COVID-19 exhibited pneumonia and

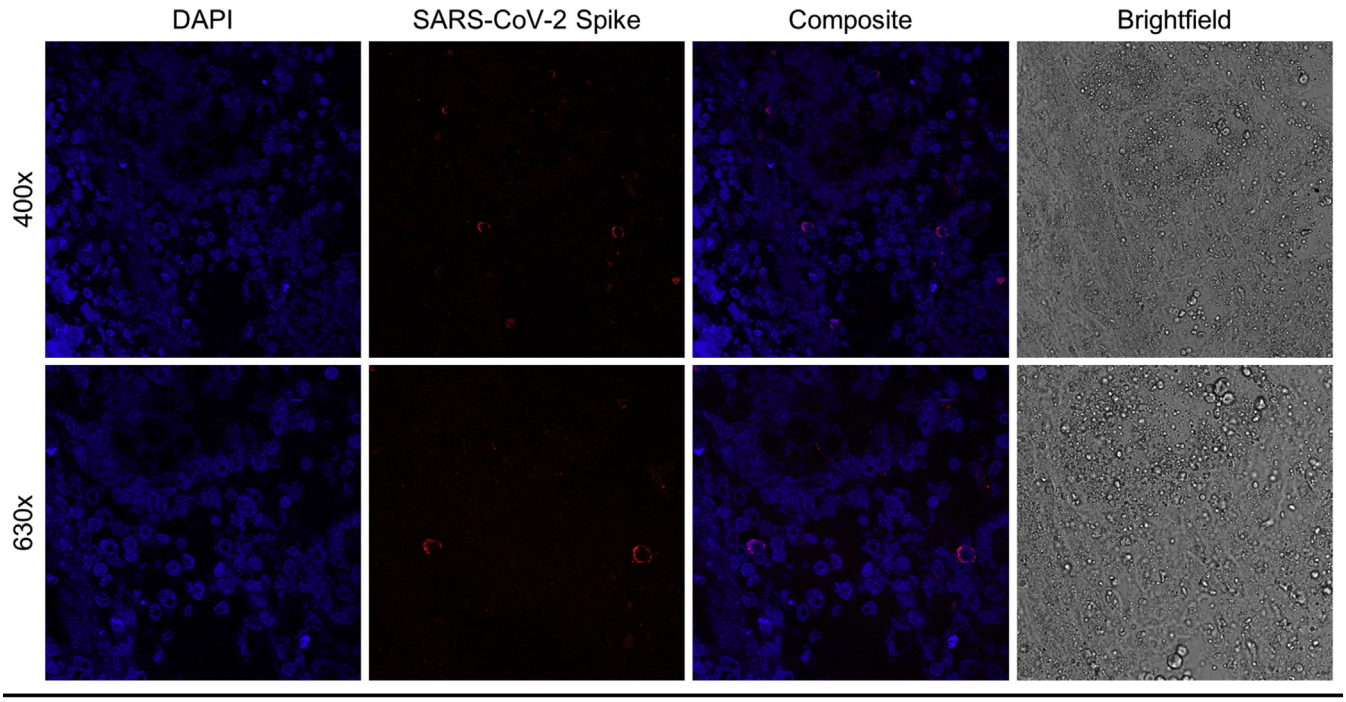

Figure 4. Immunofluorescence of cecum cells. The first column shows cell nuclei using DAPI staining. In the second and third columns, SARS-CoV-2 S (spike) protein is shown in red, demonstrating a perinuclear pattern. Images were obtained by confocal microscopy (Leica SP8) at 400 × and 630 × and processed using ImageJ.

diffuse alveolar damage, which is a hallmark in adults with COVID-19.[13,17]

In our patient, the heart showed myocarditis with significant lymphocyte and macrophage infiltrate. Autopsies of patients with MIS-C showed significant cardiac involvement, with areas of necrosis. In contrast, only myocardial interstitial edema was seen on autopsies of 2 patients with acute COVID-19 infection.[10] Gruber et al observed a reduction of peripheral blood nonclassical monocytes and subsets of T lymphocytes and natural killer cells, compatible with extravasation to affected tissues,[5] which is in accordance with the microscopic findings in our patient's heart.

The presence of complement C4d in several tissues, mainly the intestine, heart, liver, and skin is consistent with an underlying immunologic process. Duarte-Neto et al also described positive C4d immunohistochemistry in the heart.[10] The existence of hemophagocytosis in the bone marrow in our case, and in 2 of the 3 reported MIS-C cases in the spleen as well as in the liver in 1 case, also indicates significant immune activation.[10]

SARS-CoV-2 spike protein was identified in colonic cells of our patient. This finding is in accordance with a report describing that SARS-CoV-2 RNA remains in the gastrointestinal tract for weeks in children with MIS-C,[18] the severe gut inflammation in our case and in 1 child in the series of Duarte-Neto et al[10] could be related to increased permeability of the gastrointestinal mucosal barrier. The breakdown of mucosal barrier function coincides with SARS-CoV-2 antigenemia, likely instigating and driving the aberrant immune activation defining MIS-C.[18] Along with persistent antigen leakage from the gut,[19] poor antigen clearance also could play a role in MIS-C pathogenesis.[18] Carter et al reported impaired antigen presentation in this condition.[4] Furthermore, the spike protein has been hypothesized to have superantigen-like properties.[20]

Gastrointestinal symptoms are the most frequent manifestation of MIS-C along with fever.[2,16,18] The predominance of this clinical presentation, along with the finding of viral components in gut cells,[10] may suggest that the viral antigenic source is in the gut.[18] Similarly, it has been described that the gut serves as a nidus for SARS-CoV-2 in adults.[21]

In our child, SARS-CoV-2 protein S was not observed in the lungs or heart, and in the previous report, SARS-CoV-2 particles were found in the heart and lungs of all 3 children as well as in the liver, kidney, spleen, brain, and sweat glands.[10] Our demonstration of SARS-CoV-2 spike protein in intestinal cells by immunofluorescence supports the hypothesis that the gut is important in the pathogenesis of MIS-C. ■

We thank the parents who provided consent to include their children in the medical literature. We also thank Drs Santiago Melón and Marta Elena Argüelles for their help in interpreting viral findings.

Submitted for publication Sep 1, 2021; last revision received Nov 12, 2021; accepted Nov 19, 2021.

Reprint requests: Juan Mayordomo-Colunga, MD, PhD, Sección de Cuidados Intensivos Pediátricos, Área de Gestión Clínica de Pediatría, Hospital Universitario Central de Asturias, Avda, de Roma s/n 33011, Oviedo, Asturias, Spain. E-mail: jmc@crit-lab.org; jmcolunga@hotmail.com

References

1. Royal College of Paediatrics and Child Health (RCPCH). Guidance: Paediatric multisystem inflammatory syndrome temporally associated with COVID-19 (PIMS): guidance for clinicians. Accessed July 14, 2021. https://www.rcpch.ac.uk/sites/default/files/2020-05/COVID-19-Paediatric-multisystem-%20inflammatory%20syndrome-20200501.pdf
2. Bautista-Rodriguez C, Sanchez-de-Toledo J, Clark BC, Herberg J, Bajolle F, Randanne PC, et al. Multisystem inflammatory syndrome in children: an international survey. Pediatrics 2021;147:e2020024554.
3. Feldstein LR, Tenforde MW, Friedman KG, Newhams M, Rose EB, Dapul H, et al. Characteristics and outcomes of US children and adolescents with multisystem inflammatory syndrome in children (MIS-C) compared with severe acute COVID-19. JAMA 2021;325:1074-87.
4. Carter MJ, Fish M, Jennings A, Doores KJ, Wellman P, Seow J, et al. Peripheral immunophenotypes in children with multisystem inflammatory syndrome associated with SARS-CoV-2 infection. Nat Med 2020;26:1701-7.
5. Gruber CN, Patel RS, Trachtman R, Lepow L, Amanat F, Krammer F, et al. Mapping systemic inflammation and antibody responses in multisystem inflammatory syndrome in children (MIS-C). Cell 2020;183:982-95.e14.
6. Feldstein LR, Rose EB, Horwitz S, Collins JP, Newhams MM, Son MBF, et al. Multisystem inflammatory syndrome in US children and adolescents. N Engl J Med 2020;383:334-46.
7. Valverde I, Singh Y, Sanchez-de-Toledo J, Theocharis P, Chikermane A, Di Filippo S, et al. Acute cardiovascular manifestations in 286 children with multisystem inflammatory syndrome associated with COVID-19 infection in Europe. Circulation 2021;143:21-32.
8. García-Salido A, de Carlos Vicente JC, Belda Hofheinz S, Balcells Ramírez J, Slöcker Barrio M, Leóz Gordillo I, et al. Severe manifestations of SARS-CoV-2 in children and adolescents: from COVID-19 pneumonia to multisystem inflammatory syndrome: a multicentre study in pediatric intensive care units in Spain. Crit Care 2020;24:666.
9. Whittaker E, Bamford A, Kenny J, Kaforou M, Jones CE, Shah P, et al. Clinical characteristics of 58 children with a pediatric inflammatory multisystem syndrome temporally associated with SARS-CoV-2. JAMA 2020;324:259-69.
10. Duarte-Neto AN, Caldini EG, Gomes-Gouvêa MS, Kanamura CT, de Almeida Monteiro RA, Ferranti JF, et al. An autopsy study of the spectrum of severe COVID-19 in children: from SARS to different phenotypes of MIS-C. EClinicalMedicine 2021;35:100850.
11. Bigdelian H, Sedighi M, Sabri MR, Dehghan B, Mahdavi C, Ahmadi A, et al. Case report: Acute intracardiac thrombosis in children with coronavirus disease 2019 (COVID-19). Front Pediatr 2021;9:656720.
12. Dorward DA, Russell CD, Um IH, Elshani M, Armstrong SD, Penrice-Randal R, et al. Tissue specific immunopathology in fatal COVID-19. Am J Respir Crit Care Med 2021;203:192-201.
13. Vella LA, Rowley AH. Current insights into the pathophysiology of multisystem inflammatory syndrome in children. Curr Pediatr Rep 2021. https://doi.org/10.1007/s40124-021-00257-6 [Epub ahead of print].
14. Amano S, Hazama F, Kubagawa H, Tasaka K, Haebara H, Hamashima Y. General pathology of Kawasaki disease. On the morphological alterations corresponding to the clinical manifestations. Acta Pathol Jpn 1980;30:681-94.
15. Fox SE, Lameira FS, Rinker EB, Vander Heide RS. Cardiac endotheliitis and multisystem inflammatory syndrome after COVID-19. Ann Intern Med 2020;173:1025-7.
16. Carter MJ, Shankar-Hari M, Tibby SM. Paediatric inflammatory multisystem syndrome temporally-associated with SARS-CoV-2 infection: an overview. Intensive Care Med 2021;47:90-3.

17. Fox SE, Akmatbekov A, Harbert JL, Li G, Brown JQ, Vander Heide RS. Pulmonary and cardiac pathology in African American patients with COVID-19: an autopsy series from New Orleans. Lancet Respir Med 2020;8:681-6.
18. Yonker LM, Gilboa T, Ogata AF, Senussi Y, Lazarovits R, Boribong BP, et al. Multisystem inflammatory syndrome in children is driven by zonulin-dependent loss of gut mucosal barrier. J Clin Invest 2021;131:e149633.
19. Vella LA, Giles JR, Baxter AE, Oldridge DA, Diorio C, Kuri-Cervantes L, et al. Deep immune profiling of MIS-C demonstrates marked but transient immune activation compared to adult and pediatric COVID-19. Sci Immunol 2021;6:eabf7570.
20. Porritt RA, Paschold L, Rivas MN, Cheng MH, Yonker LM, Chandnani H, et al. HLA class I–associated expansion of TRBV11-2 T cells in multisystem inflammatory syndrome in children. J Clin Invest 2021;131:e146614.
21. Gaebler C, Wang Z, Lorenzi JCC, Muecksch F, Finkin S, Tokuyama M, et al. Evolution of antibody immunity to SARS-CoV-2. Nature 2021;591:639-44.

50 Years Ago in *The Journal of Pediatrics*

Serum Hepatitis and Infectious Hepatitis: One and the Same?

Dietzman DE, Matthew EB, Madden DL, Sever JL, Rostafinski M, Bouton SM, et al. The occurrence of epidemic infectious hepatitis in chronic carriers of Australia antigen. J Pediatr 1972;80:577-82.

In 1972, Dietzman et al characterized an epidemic of infectious hepatitis at a mental health institution in Lynchburg, Virginia, and sought to identify if patients with Australia antigen (Au)–contracted infectious hepatitis at differing rates than those without the antigen. "Infectious hepatitis" is described as an acute infection, transmitted by the fecal–oral route, resulting in jaundice and elevated aminotransferase levels. In contrast, "serum hepatitis" is a parenterally transmitted form of hepatitis often associated with chronic infection and the distinct serum marker "Australia antigen." Of the 3600 patients and 1600 employees at the facility, 565 cases of infectious hepatitis occurred during the institutional epidemic. Ten wards with 446 patients were included in the study group, and 51 of these patients were Au-positive. The rates of epidemic infection did not differ between the Au-positive subjects (63%) and Au-negative group (61%). The prevalence of Au was greater in patients <15 years old and in patients with trisomy 21. The key message is that "serum hepatitis" and "infectious hepatitis" are immunologically unrelated and caused by different etiologic agents.

This article provides an intriguing perspective on the progress of research in viral hepatitis over the past 50 years. The "Australia antigen," discovered in 1965 by Dr Baruch Blumberg, is known today as hepatitis B surface antigen.[1] "Infectious hepatitis" is a distinct infection, identified in 1973 as the hepatitis A virus. Indeed, chronic infection with hepatitis B is not protective against hepatitis A infection. Greater prevalence of hepatitis B surface antigen in younger patients with normal aminotransferase levels likely indicated the immune-tolerant phase of perinatally transmitted hepatitis B. The notion that patients with trisomy 21 have greater rates of chronic hepatitis B was later disproven and was likely explained by greater infection rates in institutionalized settings.[2]

Currently, the focus has shifted to prevention of hepatitis A virus and hepatitis B virus infection (vaccination) and treatment of the latter. In utero and perinatal transmission remains the most common mode of hepatitis B infection in the pediatric population; infections acquired in infancy present high risk for progression to chronic hepatitis.[3] Screening for, and treating, hepatitis B in pregnancy and newborn administration of hepatitis B immune globulin and hepatitis B vaccination has significantly decreased rates of pediatric chronic hepatitis B. In 2019, the World Health Organization estimated that the percentage of children <5 years with chronic hepatitis B virus was reduced to <1%.[4] Despite this encouraging trajectory, research and advocacy must continue to eradicate hepatitis B—pediatricians can play a critical role.

Sindhu Pandurangi, MD
Division of Gastroenterology, Hepatology and Nutrition
Cincinnati Children's Hospital Medical Center
Cincinnati, Ohio

References

1. Blumberg BS, Alter HJ, Visnich S. A "new" antigen in leukemia sera. JAMA 1965;191:541-6.
2. Madden DL, Matthew EB, Dietzman DE, Purcell RH, Sever JL, Rostafinski M, et al. Hepatitis and Down's syndrome. Am J Ment Defic 1976;80:401-6.
3. Hsu H-Y, Chang M-H. Hepatitis B virus infection and the progress toward its elimination. J Pediatr 2019;205:12-20.
4. World Health Organization. Hepatitis B [Fact Sheet]. 2021. Accessed January 4, 2022. https://www.who.int/en/news-room/fact-sheets/detail/hepatitis-b

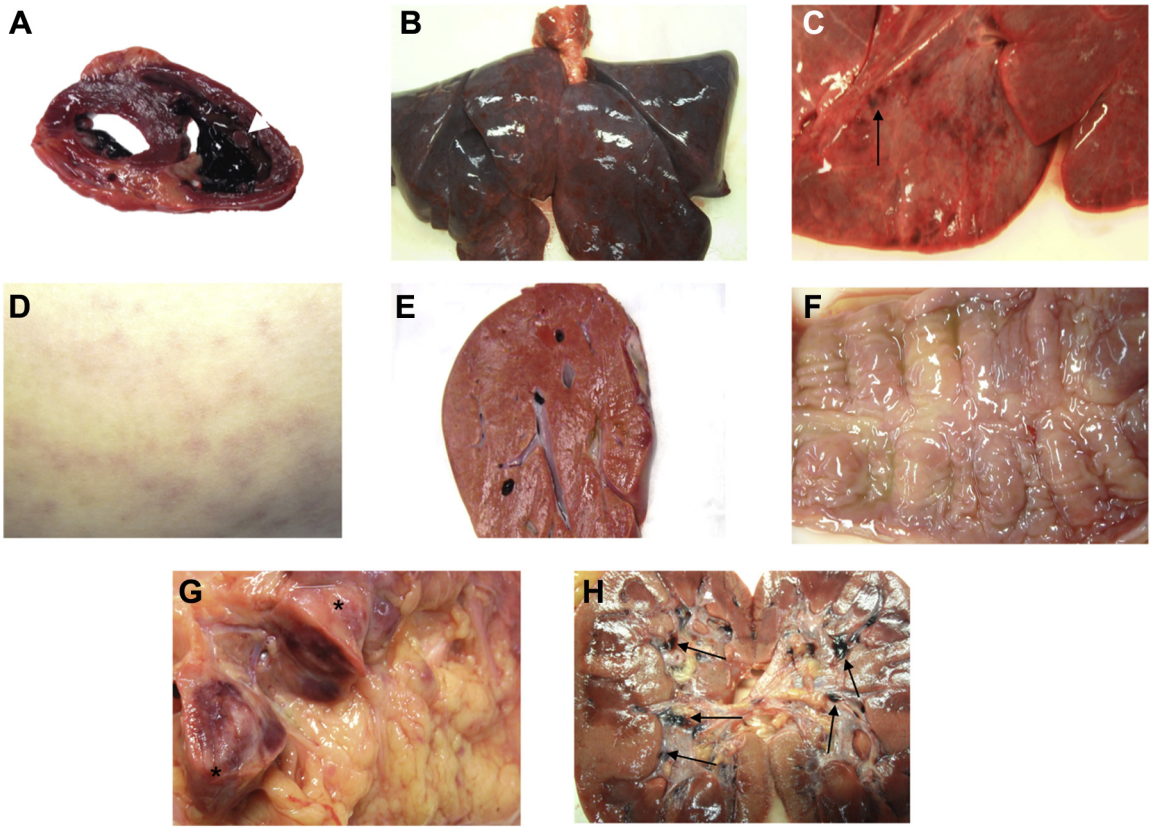

Figure 1. The most relevant macroscopic findings. **A**, Nondilated heart showing a 4 × 1 cm thrombus in the right ventricle (*white arrow*), encircling a papillary muscle. Coronary arteries were patent. **B** and **C**, Severely congested lungs, showing petechiae on the external surface. No thrombi were found in the pulmonary artery and main branches. **D**, Dorsum showing a rash. **E**, Congested liver. **F**, Edematous cecum mucosa. **G**, A 9 × 2.5 cm lymphadenopathy (*asterisks*) found next to the cecum, showing extensive areas of hemorrhage on cut sections. **H**, Kidneys showing multiple clots in calices (*black arrows*).

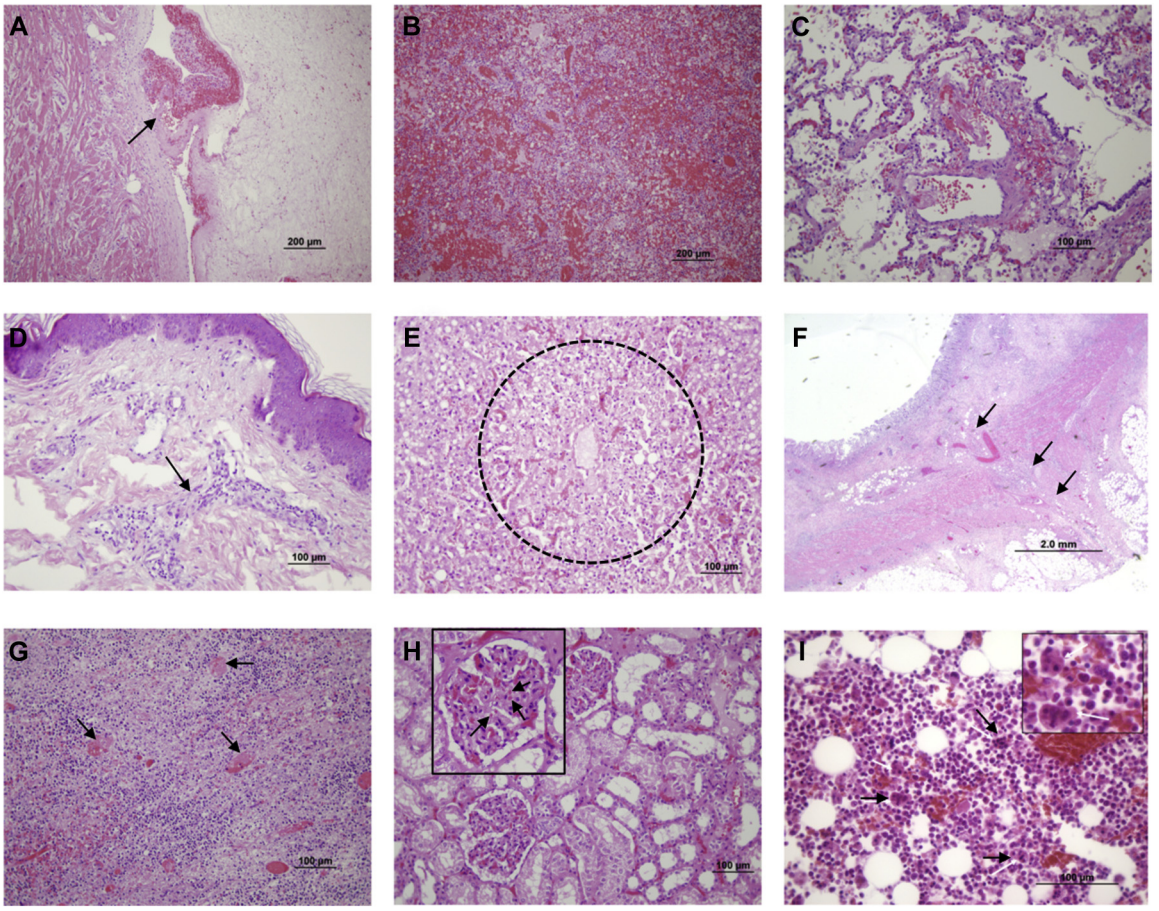

Figure 2. The most relevant microscopic findings. Formalin-fixed, paraffin-embedded tissue blocks were processed and hematoxylin and eosin–stained after a standardized process in the hospital pathology laboratory. **A**, Organized cardiac thrombus, adhered to the ventricular wall (*arrow*). **B**, Intense pulmonary hemorrhage. **C**, Thrombi in pulmonary microvasculature (*arrows*). **D**, Perivascular inflammatory cells (*arrow*) in the skin (rash area on the dorsum). **E**, Centrilobular necrosis in the liver (30%-40% of the liver exhibited this pattern). **F**, Pericecal adenopathy showing intense necrosis secondary to thrombi (*arrows*). **G**, Transmural chronic inflammation in the cecum. **H**, Thrombi in glomerular microcirculation; the square shows a glomerulus in detail, with microthrombi (*arrows*). **I**, Hemophagocytosis (*arrows*) in bone marrow aspirate.

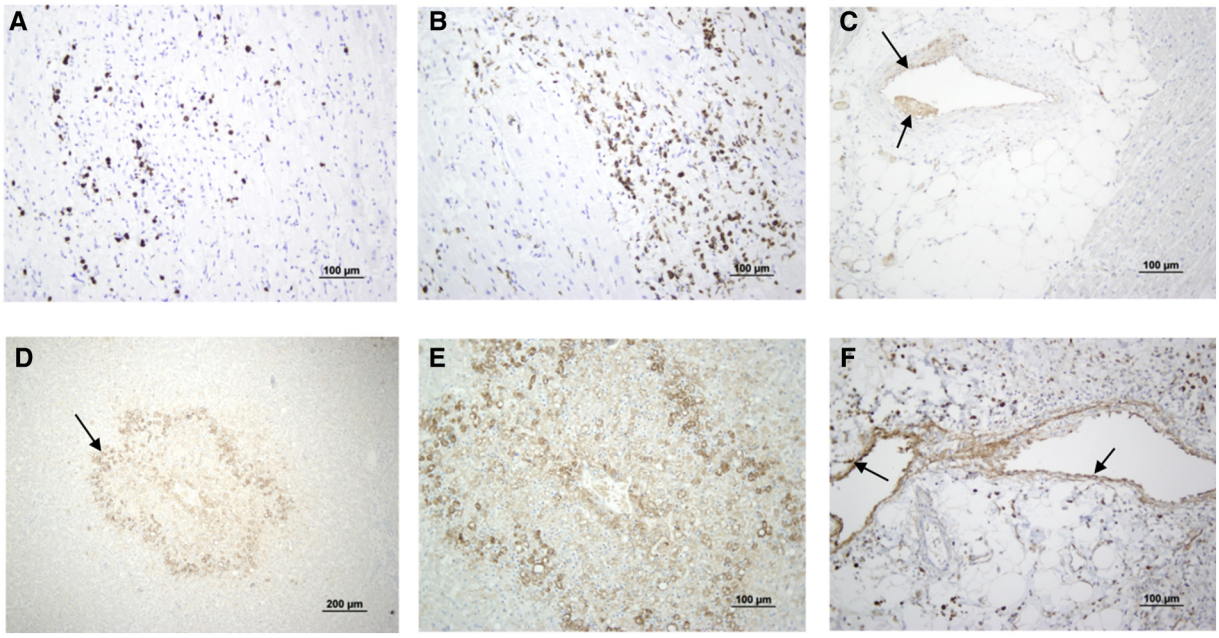

Figure 3. Immunohistochemistry of several organs. Infiltration of the heart with **A**, $CD3^+$ T lymphocytes and **B**, $CD68^+$ macrophages. **C**, Complement C4d deposits in heart arterioles. **D** and **E**, Complement C4d deposits in the liver, mainly in zone 3 of the lobule. **F**, Complement C4d deposits in cecum subserous fat tissue arterioles.

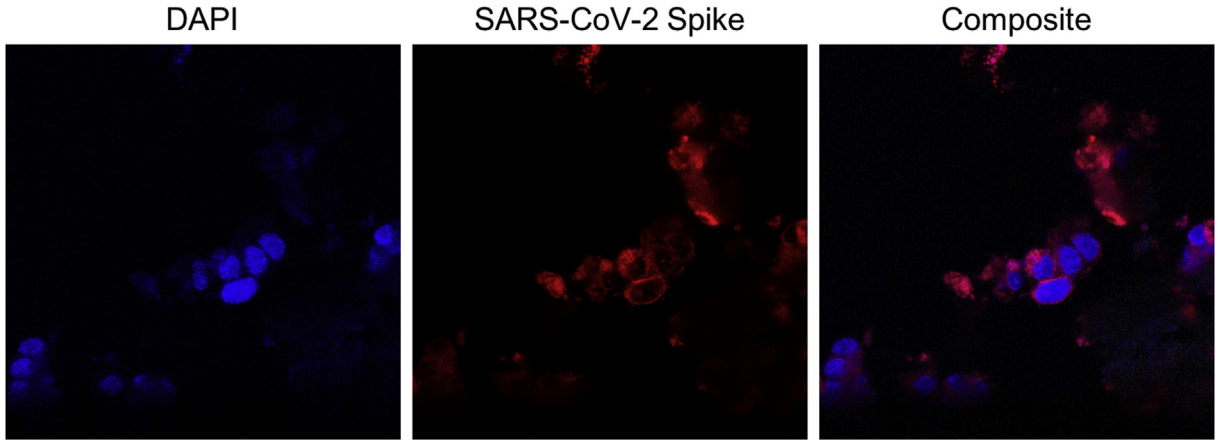

Figure 5. Immunofluorescence of pharyngeal cells inoculated with SARS-CoV-2. Images were obtained by confocal microscopy (Leica SP8) at 400 × and 630 × and processed using ImageJ. The first photograph shows cell nuclei using DAPI staining. In the second and third photos, SARS-CoV-2 S (spike) protein are shown in red, demonstrating a perinuclear pattern. The same protocol described in **Figure 3** was used to perform immunofluorescence. In this case, pharyngeal cells inoculated with SARS-CoV-2 were smeared and fixed with acetone.

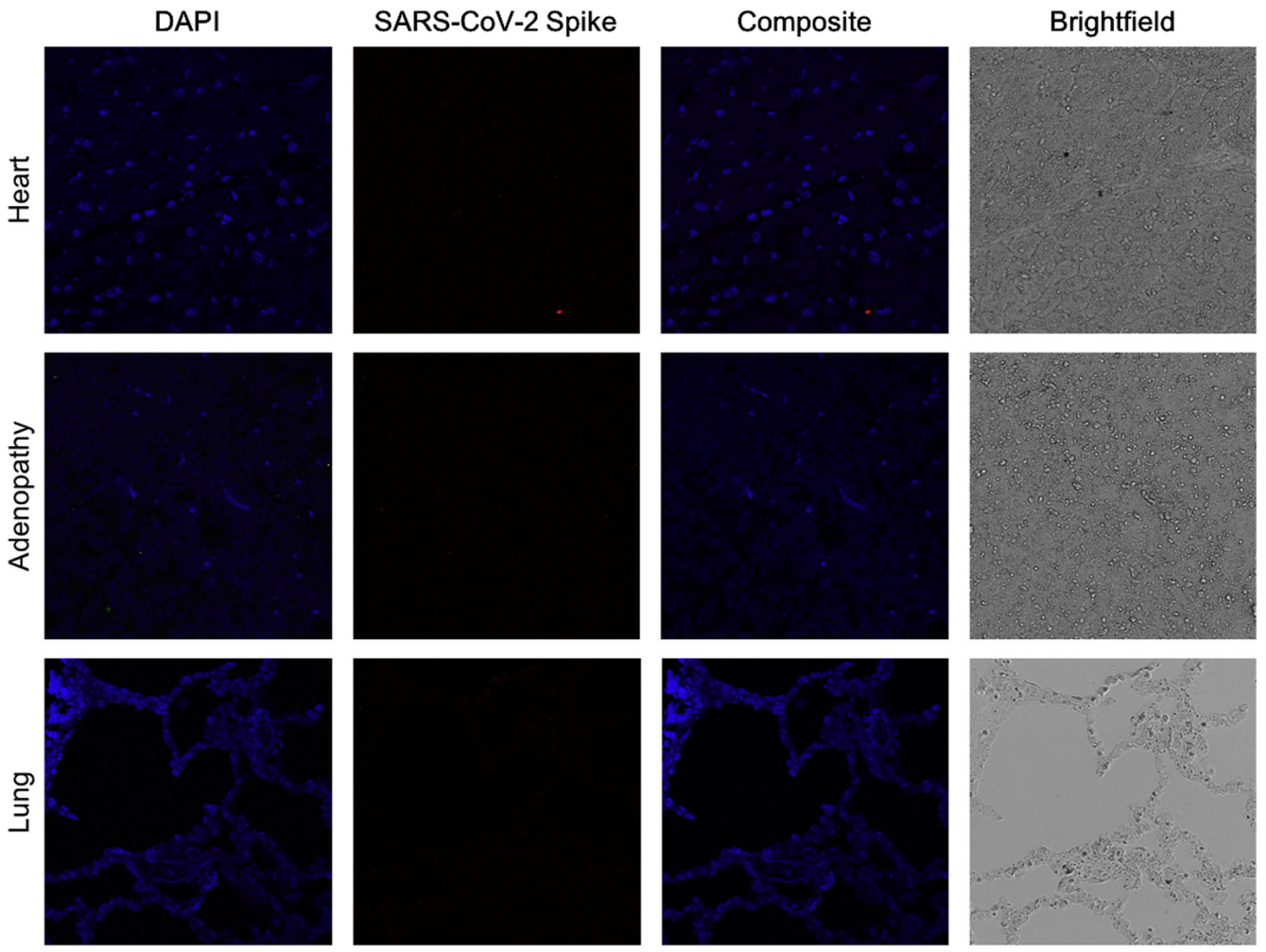

Figure 6. Immunofluorescence of the child's other organs. The first column shows cells nuclei using DAPI staining. SARS-CoV-2 S (spike) protein was not observed, as shown in the second and third columns. Images were obtained by confocal microscopy (Leica SP8) at 400 × and 630 × and processed using ImageJ. The same protocol described in **Figure 3** was used to perform immunofluorescence.

Table I. Hematologic and biochemical markers obtained during admission

Markers	Hospital admission (−15 h)	PICU admission (0 h)	+10 h	+18 h	+28 h	+40 h
Hematologic measures						
Hemoglobin, g/dL	12.2	11.1	11.4	10.3	10	—
Platelets, $10^3/\mu L$	133	131	233	242	143	—
Leukocytes/μL	8540	10 360	31 110	17 110	4290	—
Neutrophils/μL	7450	9420	28 700	15 500	3700	—
Lymphocytes/μL	510	440	1010	1110	470	—
D-dimer, ng/mL	—	2818	3045	2538	11 358	18 219
Fibrinogen, mg/dL	1224	799	840	779	532	340
Biochemical parameters						
C-reactive protein, mg/dL	28.7	31.6	33.4	27.7	22.4	16.8
Procalcitonin, ng/mL	6.75	6.18	23.1	83.8	225	>800
IL-6, pg/mL	515	459	486	121	—	43
Ferritin, ng/mL	—	871	—	—	—	—
NTproBNP, pg/mL	—	14 398	31 788	35 965	—	>70 000
Cardiac troponin T, ng/L	—	161	360	370	495	1059
Sodium, mmol/L	134	136	139	142	142	143
Potassium, mmol/L	3.9	—	3.2	2.8	3.1	4.9
Urea, mg/dL	23	42	46	49	71	102
Creatinine, mg/dL	0.57	0.7	1.08	1.01	1.76	3.25
Albumin, g/L	—	30	31	31	26	24
AST, U/L	124	87	64	143	1908	5220
ALT, U/L	138	104	92	107	844	1913
LDH, U/L	372	—	—	549	3980	6180
Lactate, mmol/L	—	2.7	9.3	2.4	2.8	3.5

ALT, alanine aminotransferase; *AST*, aspartate aminotransferase; *IL-6*, interleukin 6; *LDH*, lactate dehydrogenase; *NTproBNP*, N-terminal pro B-type natriuretic peptide.